Data Mining Classifiers for Real Time Power Quality Disturbance Signal Analysis incorporating Wavelet Features

4

S. Upadhyaya Department of Electrical Engineering
SUIIT, Burla, Sambalpur-768019, India

Abstract

In this paper, Maximal overlap discrete Wavelet Transform (MODWT) has been implemented along with the traditional discrete wavelet transform (DWT) for the detection and localization of different types of power quality (PQ) disturbance signals. Each of the signal has been decomposed up to fourth level with both the MODWT and DWT. The co-efficients of both MODWT and DWT decomposition have been further used for classification. The selected features have been extracted from the detail coefficient of the variants of WT and then given as inputs to the data mining classifiers for characterization of the signals. Moreover, a comparative assessment of the PQ signal has been carried out with different classifiers such as Decision Tree (DT) and Random Forest (RF) have been implemented along with aforementioned detection techniques. The ensemble decision tree named RF has been used for the classification of large number of data set. Various single as well as combined power quality disturbance signals have been simulated in noisy and noise free environment in order to demonstrate the efficiency of the proposed techniques. Moreover, in order to represent in realistic environment, these techniques have been tested with tree phase signals captured from transmission line panels.

I. Introduction

The Power Quality disturbance (PQD) study has become an important aspect in the area of power system, as these disturbances affect the overall harmony of the system. Ordinarily, an AC voltage waveform and AC current waveform are expected to be sinusoidal at the system frequency. But there are several factors, namely the use of solid state devices, equipment failure etc., which deviates deviates the waveform from being a sinusoid [1]. Due to these circumstances the quality of power deteriorates, which brings instability in the power system. The deviated waveforms could be a sag waveform,oscillatory transient waveform, waveform swell etc. Hence, in order to maintain a healthy and a stable system, it is important to maintain the voltage profile in terms of improvement of the quality of power.

First of all, the detection and the localization of the various types of PQ disturbance are required before going for improvement of voltage profile. In order to identify the disturbances, the different techniques such as the Fourier transform (FT), the short-time Fourier transform (STFT), wavelet transform (WT), Neural Network, Fuzzy logic, S-transform have been used [2], [3]. The FT gives the information about the frequency component only. On the other hand, the time frequency information related to the disturbance waveform can be obtained by implementing STFT [4]. However, STFT is fails to track the transient signals perfectly due to its fixed window property [5]. Similarly, the S-transform suffers from computational burden [6]. The wavelet transform affords the time-scale analysis of the non-stationary signal due to Multi-Resolution Analysis (MRA) property. The property of MRA represents the signals into different time-scales. The WT provides time-frequency information by the dilation and translation of the wavelet with the signal.

In this paper, the variants of WT namely the maximum overlapping discrete Wavelet Transform (MODWT) [7], [8], [9] and the traditional DWT are implemented for the feature extraction of the PQ disturbances. The extracted features from the decomposition of WT are used for classification of the PQ signals.

The accurate detection of the PQ disturbance is the important performance indices in power quality analysis. However, the most common automated classification models are based on the Artificial Neural Network (ANN)

[10], fuzzy and neuro-fuzzy systems [11]. But the main disadvantage of ANN based classifier is the requirement of retraining when a new phenomenon is added. Moreover, the Hidden Markov Model (HMMs) classifier is not suitable to classify the slow phenomena like interruption [12], [13]. Similarly the decision tree (DT) is a good classifier [14] but it suffers with over fitting problem when large number of classes are to be classified [15]. In this paper, Decision Tree (DT) [16], [17] and Random Forest (RF) have been implemented to discriminate the PQD signals in order to establish a comparative assessment of MODWT application in PQ environment.

The Random forest (RF) is good candidate in the area of classification. However, the RF simultaneously classifies both the fast and slow phenomena.

This paper organized as follows. The Section-II describes the theory of the MODWT along with the DWT. The feature extraction processes are presented in the Section-III. Section-IV provides the brief theory about the classifiers. Similarly, the Section-VI deals with the construction of PQ model as well as the effectiveness of MODWT and DWT in the detection as well as localization of the PQ disturbances. The classification results are presented in the Section-VII. Finally, Section-VIII provides the concluding remark.

II. Localization Approach

The detection of the PQ disturbance has been carried out by implementing the variants of wavelet transform i.e DWT and the MODWT. These techiques are briefly described in this section while the feature extraction and classification are described in the subsequent sections.

A. Continuous Wavelet Transform

The wavelet transform represents the signal as a combination of the wavelets at different location and scales. The continuous wavelet transform generally implements for analysis of the continuous time signal. The surface of the wavelet coefficients is obtained from the different values of the scaling and the translation factors. Mathematically, for a signal $x(t)$, the continuous wavelet transform [18] can expressed

$$CWT(a,b) = \frac{1}{\sqrt{a}} \int_{-\infty}^{\infty} x(t)\, g\left(\frac{t-b}{a}\right) dt \tag{1}$$

where $g(\cdot)$ is the mother wavelet. Similarly, a is the scale factor and b is the translation factor. Both a and b are varies in continuous manner. In order to eliminate the redundancy due to continuous coefficients, discrete Wavelet transform has been introduced which has been discussed in next subsequent subsection.

B. Discrete Wavelet Transform

The discrete wavelet transform (DWT) implements to decompose a discretized signal into different resolution levels. The DWT reduces the substantial redundancy of CWT. The multiresolution analysis (MRA) of the wavelet function generates the detail coefficients of the decomposed signal whereas the scaling function generates the approximation coefficients. The DWT can be expressed with g as the mother wavelet as

$$DWT(m,k) = \frac{1}{\sqrt{a_0^m}} \sum_n x(n)\, g\left(\frac{k - n b_0 a_0^m}{a_0^m}\right) \tag{2}$$

where k is an integer which stands for the sample reference. The scaling parameter and the translation parameter a and b vary in the discrete manner. The time signal $S[n]$ decomposed in to detailed $d_1(n)$ and smoothed $c_1(n)$ version by employing high pass $(h(n))$ and low pass filters $(l(n))$ called as 'Quadrature mirror filters'. Thus the detail version contains high frequency components than the smooth version. $c_1(n)$. Mathematically, they are specified [19] as

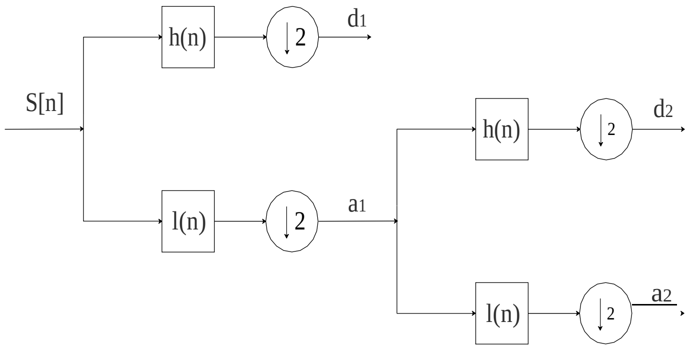

Fig. 1: Block diagram of DWT decomposition

$$c_1(n) = \sum_k h(k-2n)c_0(k) \tag{3}$$

$$d_1(n) = \sum_k g(k-2n)c_0(k) \tag{4}$$

where $c_0(n)$ is the discretised time signal (sampled version of $S_0(n)$). The outputs of the two filters are down sampled by a factor of 2 in order to obtain the DWT coefficients. The output of the low pass filter is called the approximation coefficients and the output of the high pass filter is called as the detail coefficients. The approximation coefficients are further fed to the low pass and high pass filter in ordered to iterate the analysis process. The Quadrature mirror filters are related by the equation

$$h[L-1-n] = (-1)^n l(n) \tag{5}$$

where, L is the filter length. The signal which is fed to both the low pass and high pass filter is shown in Fig.1.

The implementation of DWT is restricted with the length of signals. Similarly, the coefficients are affected by the change of initial point. So modified DWT (MODWT) has been implemented in ordered to overcome the drawbacks of the DWT which is presented in the subsequent subsection.

C. Maximum Overlapping Discrete Wavelet Transform (MODWT)

The motivation to formulate the MODWT over the conventional DWT is the ability of the free selection of a starting point of a time series signal. The orthogonal transform of DWT suffers from the lack of the invariance translation in time series analysis. The Maximum Overlap Discrete Wavelet Transform is the enhanced version of the Discrete Wavelet Transform (DWT). This transform can be employed to any sample size whereas the DWT is limited to the signal length N to be an intermultiple of 2^j where $j = 1, 2, 3, \ldots, J$ is the scale number [9]. The representation of MODWT is shown in Fig.2. The MODWT scaling filter $\tilde{h}_l$ and the wavelet filters g_l are related to the DWT filters through (6) and (7)

h_l

$$\tilde{h}_l = \frac{h_l}{\sqrt{2}} \tag{6}$$

$$\tilde{g}_l = \frac{g_l}{\sqrt{2}} \tag{7}$$

The MODWT filters are also in the quadrature mirrors like DWT filter is given as (9) and (8)

$$\tilde{g}_l = (-1)^{l+1}\,\tilde{h}_{L-1-l} \tag{8}$$

$$\tilde{h}_l = (-1)^{l}\,\tilde{g}_{L-1-l} \tag{9}$$

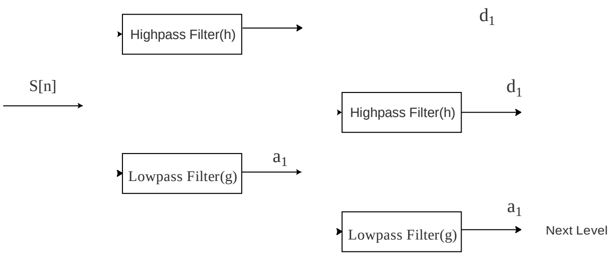

Fig. 2: Block diagram representation of MODWT decomposition

where $l = 0, 1, 2, ..., L-1$ and L is the width of the filter.

The n^{th} element of the first-stage wavelet and the scaling coefficients of MODWT with the input time series signal $X(n)$ is as follows

$$\widetilde{W}_{1,n} = \sum_{l=0}^{L-1} \tilde{h}_l X_{n-l \bmod N} \quad (10)$$

$$\widetilde{V}_{1,n} = \sum_{l=0}^{L-1} \tilde{g}_l X_{n-l \bmod N} \quad (11)$$

where $n = 1, 2, 3, ..., N$ and N is the length of signal in sample.

$$\widetilde{A}_{1,n} = \sum_{l=0}^{L_1-1} \tilde{g}_l \widetilde{V}_{1,n+l \bmod N} \quad (12)$$

$$\widetilde{D}_{1,n} = \sum_{l=0}^{L_1-1} \tilde{g}_l \widetilde{W}_{1,n+l \bmod N} \quad (13)$$

The first-stage approximations and details can be calculated by the equations (12) and (13). The MODWT scaling coefficients $\widetilde{V}_j$ and W_j wavelet coefficients at the n^{th} element of the j^{th} stage are given by the equations (14) and (15)

$$\widetilde{V}_{j,n} = \sum_{l=0}^{L_j-1} \tilde{g}_{j,1} X_{n-l \bmod N} \quad (14)$$

$$\widetilde{W}_{j,n} = \sum_{l=0}^{L_j-1} \tilde{h}_{j,1} X_{n-l \bmod N} \quad (15)$$

Similarly, the approximations $\widetilde{A}_j$ and the details $\widetilde{D}_j$ of the n^{th} element of the j^{th} stage MODWT are given by the equations (16) and (17).

$$\widetilde{A}_{j,n} = \sum_{l=0}^{L_j-1} \tilde{g}^0_{j,l} \widetilde{V}_{j,n+l \bmod N} \quad (16)$$

$$\widetilde{D}_{j,n} = \sum_{l=0}^{L_j-1} \tilde{h}^0_{j,l} \widetilde{W}_{j,n+l \bmod N} \quad (17)$$

where $\tilde{g}^0$ is periodized $\tilde{g}$ to length N and also the $\tilde{h}^0$ is periodized $\tilde{h}$ to length N. So the original time series

5

$l=0$

l l

signal can be stated in terms of the approximations and the details as follows

$$X(n) = \sum_{l=0} \tilde{D}_j + \tilde{A}_j \qquad (18)$$

The original signal can be synthesized easily from the decomposed signals like the traditional DWT and FT techniques. The DWT and proposed MODWT has been implemented in the subsequent Section.

III. Theory of the Feature Extraction

A. Feature extraction

The detail and the approximation coefficients are not directly fed as input to the classifiers. So, the feature extraction is carried out with approximation and detail coefficients in order to reduce the dimensions of the input feature matrix. Four selected features such as the energy [20], the standard deviation [1], the entropy [21] and the CUSUM have been extracted from the detail coefficients and are given below [22] .

$$\text{Energy} \quad ED_i = \frac{1}{N}\sum_{j=1}^{N} |D_{ij}|^2 \tag{19}$$

$$\text{Standard deviation} \quad \sigma_i = \left(\frac{1}{N}\sum_{j=1}^{N} (D_{ij} - \mu_i)^2\right)^{\frac{1}{2}} \tag{20}$$

$$\text{Entropy} \quad ENT_i = -\sum_{j=1}^{N} D_{ij}^2 \log(D_{ij}^2) \tag{21}$$

$$\text{CUSUM} \quad CM_i = \sum_{j=1}^{N} (D_{ij} - \mu_i)^2 \tag{22}$$

where Mean $\mu_i = \frac{1}{N}\sum_{j=1}^{N} D_{ij}$, $i = 1, 2, 3, \ldots, l$ (level of decomposition) and N is the number of samples in each decomposed signal. In [1], disturbance signals like sag, swell, sag with harmonic and swell with harmonic has been classified using the standard deviation curve, some other signals has to classify properly. So the extracted parameters have been further fed to the data mining based classification algorithm for proper characterisation of the signals. Moreover, features are normalised with the maximum value. The classification algorithms are discussed in the subsequent section.

IV. Classification Approach

The extracted features have been give as inputs to the classifier such as the DT and the RF.

A. Decision Tree Classifier (DT)

The DT is one of the machine learning techniques in which the design process is like a binary tree structure. DT is much faster than the ANN and SVM [23] and [24]. The optimum features extracted from the training patterns are used to formulate the decision tree (DT) based classifier [25]. The construction of DT algorithm is presented below [16], [17], [26].

1) Start at a single root node.
2) Split the data set (node) into two subsets (child node) with optimal criteria.
3) If it reaches the stopping criteria, exit (called the leaf node). Otherwise, repeat step 2 to each child node to get leaf node. These leaf nodes contain the 'decisions' for classification.

The splitting criteria uses the information gain, which is based on concept of disorderliness in terms of entropy.

1) Limitation of the Decision Tree:

1) DT is extremely sensitive to small perturbations in the data set considered for the analysis. 5
2) When there are lot of un-correlated variables, the efficiency of the DT decreases.
3) Some times DT suffers from over fitting in order to classify large number of classes simultaneously.

Though widely used DT has become a good classifier than the neural network and the fuzzy logic, the ensemble

DT is called as the RF has the capability to classify large number of classes simultaneously. The RF successfully overcomes the over fitting problem of the DT .

B. Random Forest (RF)

Random forest is developed by Leo Breiman [27]. The ensemble decision tree, RF which fits many classification trees to a data set and then combines the prediction from all the correlated trees. Each tree in RF depends on the value of a separately sampled random vector. The instability of individual trees in DT is resolved in RF as they gain relatively low bias when grown adequately.

The basic block diagram of a RF, ensembled with n number of trees has been shown in Fig. 3. The basic construction of RF starts for k^{th} tree of n^{th} number of trees in the RF with the generation of a random vector ψ_k which is independent of past random vectors $\psi_k \ldots \psi_{k-1}$ with the same distribution. A single tree has grown with the training set ▮ and the set of attributes present in ψ_k, resulting in a classifier $C_k\ (p,\ \psi_k)$ with an input vector p. Moreover in random split selection, ψ consists of a number of random integers n_{try}. Each tree in RF classification caste a vote for most popular class at input p. The algorithm of RF is carried out using the following steps.

1) For $k = 1$ to n_{tree} .
    a) Draw n_{tree} bootstrap samples from the training set ▮.
    b) Grow an RF tree $C_k\ (p,\ \psi_k)$ to the bootstrapped data, by recursively iterating the steps for each terminal node of the tree until there is no possibility of further split. (Unpruned tree of maximal depth)
        i) Select n_{try} variables from the features.
        ii) Pick the best variable/split point among the n_{try}.
        iii) Split the node into two daughter nodes.
2) Output the ensemble of trees. $\{C_k\ (p, \psi_k)\ , k = 1, \ldots, n_{tree}\}$

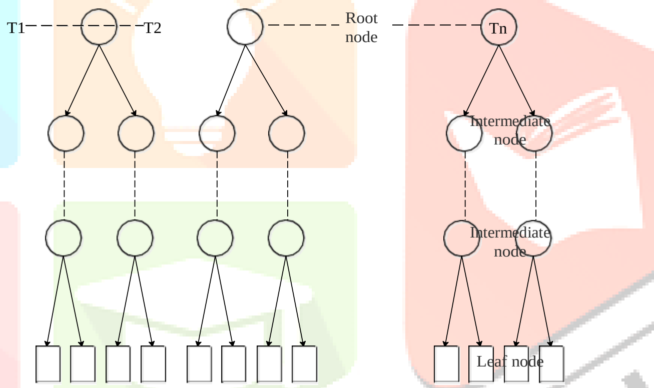

Fig. 3: Structure of RF

V. POWER QUALITY DISTURBANCE MODEL

The theory described in Section-II has been implemented in ordered to compute the approximation and detail coefficients up to fourth finer levels applying the DWT and MODWT. The PQD signals has been simulated with sampling frequency is 3.2 kHz [28]. The assigned class labels to PQ disturbances of synthesized signals has been given in Table I.

VI. DECOMPOSITION OF PQ SIGNALS

A. Pure Sinusoidal Voltage Signal

A pure sinusoidal wave of voltage signal is considered in Fig.4. With DWT and MODWT, the signal is decomposed up to four decomposition levels are shown in Fig.4 along with the original sine wave. The the vertical axis represents the amplitude of voltage signal in volt V p.u. (per unit) and similarly the horizontal axis presents the time (in second) in terms of samples. Both DWT and MODWT are implemented on the aforementioned PQ signals in order to carry out the analysis.

By decomposing normal voltage, similar types of waveforms are produced at the respective decomposition level both in DWT and the MODWT present in Fig. 4 along with the original waveform. In MODWT, the initial point is shifted due to circular shifting which helps in future prediction. The decomposition levels and the corresponding description of the pure sine wave with sag and swell are shown in Fig. 5 and Fig. 6 respectively.

TABLE I: Class labels of synthesis signal

PQD events	Class
Sag	CL1
Swell	CL2
Interruption	CL3
Oscillatory transient	CL4
Flicker	CL5
Harmonics	CL6
Sag + HarmonicsCL7	Swell
+ Harmonics	CL8
Notch	CL9
Spike	CL10

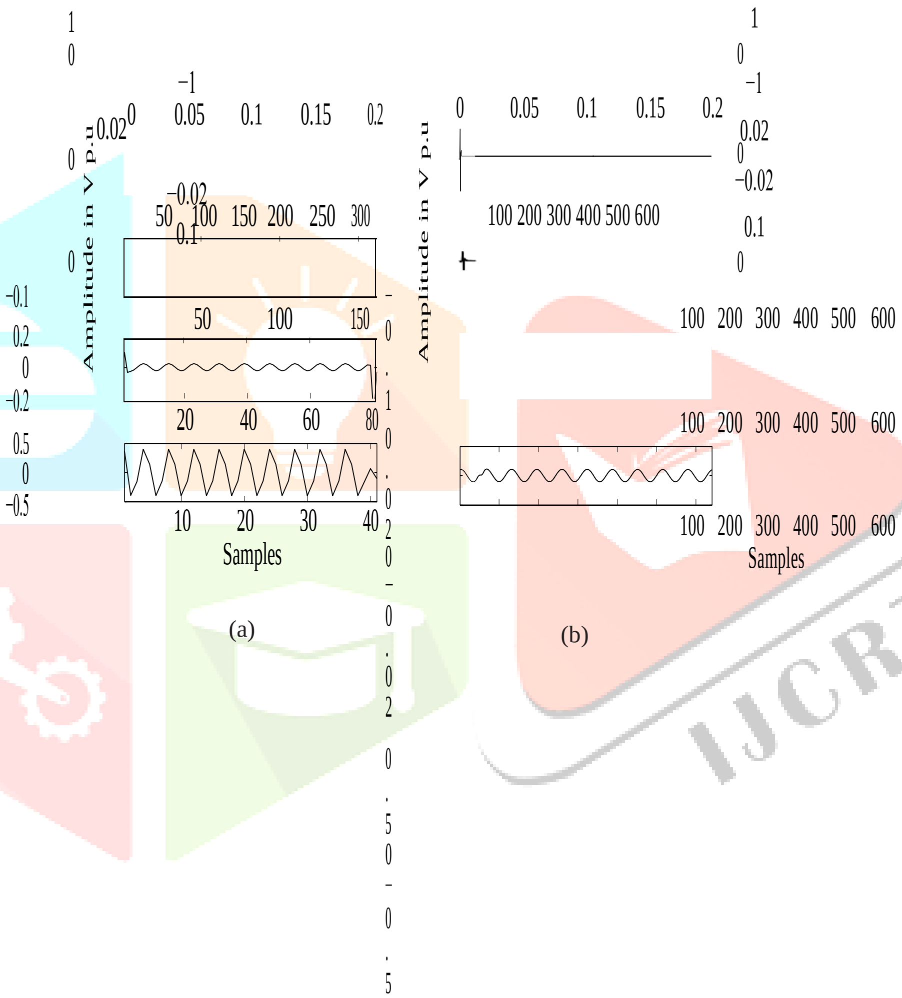

Fig. 4: Localization of pure sine wave in (a) DWT decomposition (b) MODWT decomposition

B. Pure sine wave with sag

Pure sine wave with sag has been considered for analysis. In Fig. 5, sag detection can be observed at levels 1, 2, 3 and 4. In DWT decomposition, the starting and the end point of the distortion of each decomposition level are at same alignment with the original signal, however in MODWT decomposition the first decomposed level is at the alignment with the original signal but the others are shifted due to the circular shifting.

From the Fig. 5, it is observed that, both the DWT and the MODWT decomposition provided similar type of waveforms along with the shifting.

C. Pure sine wave with swell

The procedure adopted for this type of signal is the same as the previous case. In Fig. 6, similar types of waveforms have been found in the same decomposition levels.

Similarly, the rest PQ disturbances are subjected to the process of decomposition using the DWT and the MODWT. Similar types of waveforms has been also obtained from both the types of the wavelet transforms.

In decomposition levels other than the 1st, the initial point of the signal is also sifted along with the distortions. So, MODWT can be implemented to predict the occurrence of power quality distortions.

5

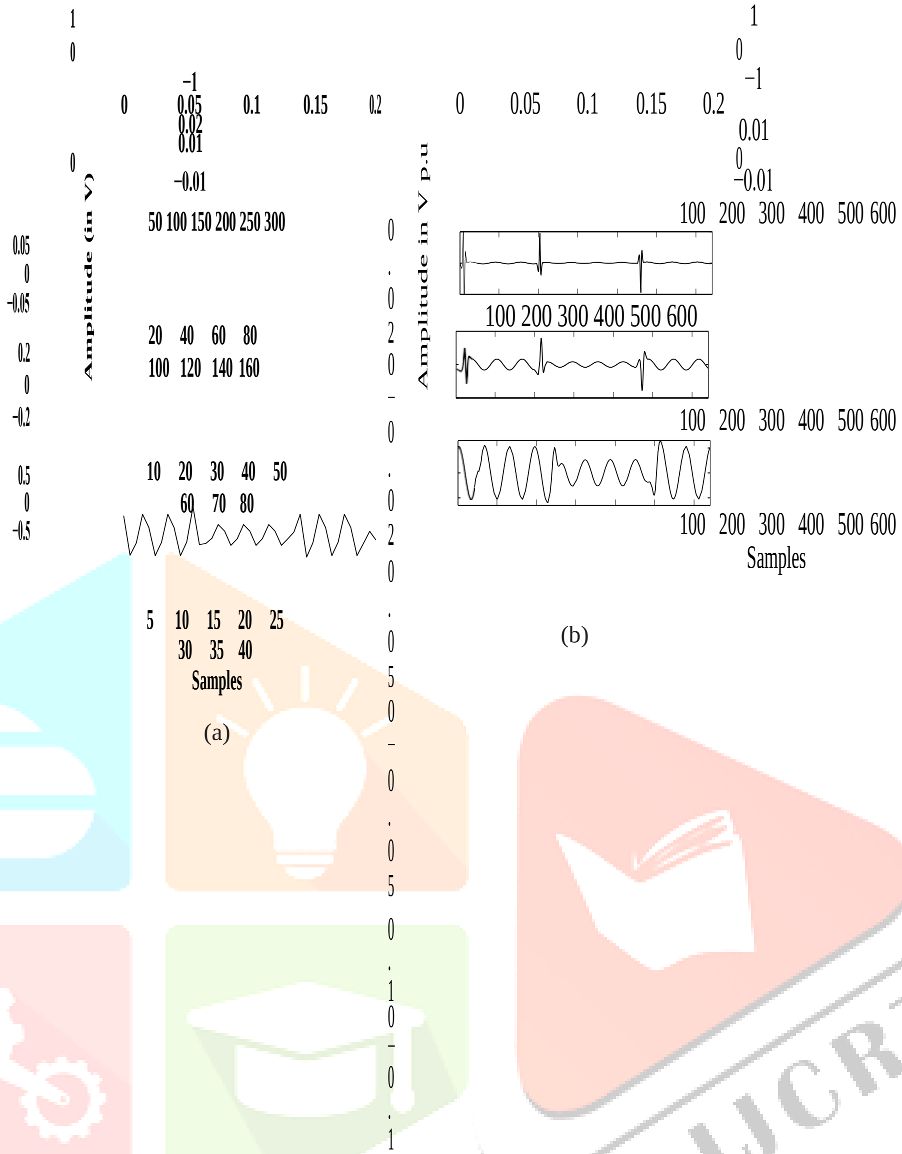

Fig. 5: Localization of sine wave with sag in (a) DWT decomposition (b) MODWT decomposition

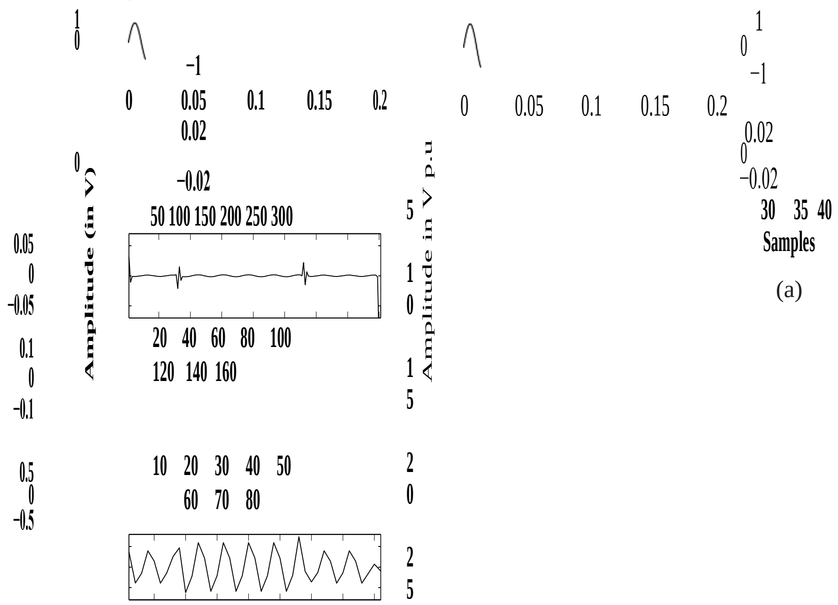

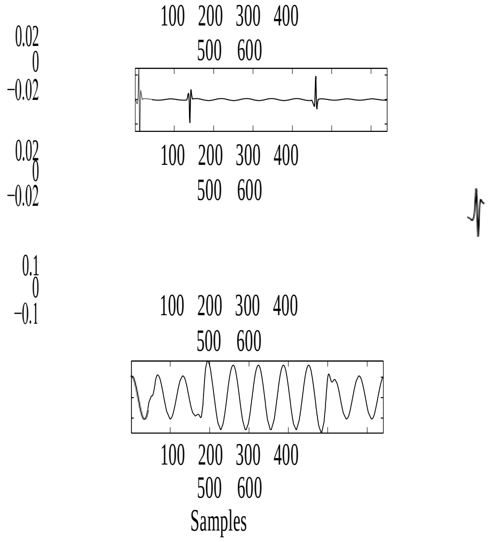

(b)

Fig. 6: Localization of sine wave with swell in (a) DWT decomposition (b) MODWT decomposition

D. Harmonic voltage signal

Consider the harmonic signal shown in Fig. 7. By observing 1st two levels of Fig. 4 and Fig. 7, it can be observed that for sinusoidal signal the magnitude of 1st two levels are almost zero and for harmonic signal, 1st two levels have some magnitude. Hence, it can be concluded that the waveforms of each level are different for different disturbance and this property helps in classification of those disturbances. Similar to that of other cases, the origin point of signals are shifted along with the distortion in the decomposition levels of MODWT.

5

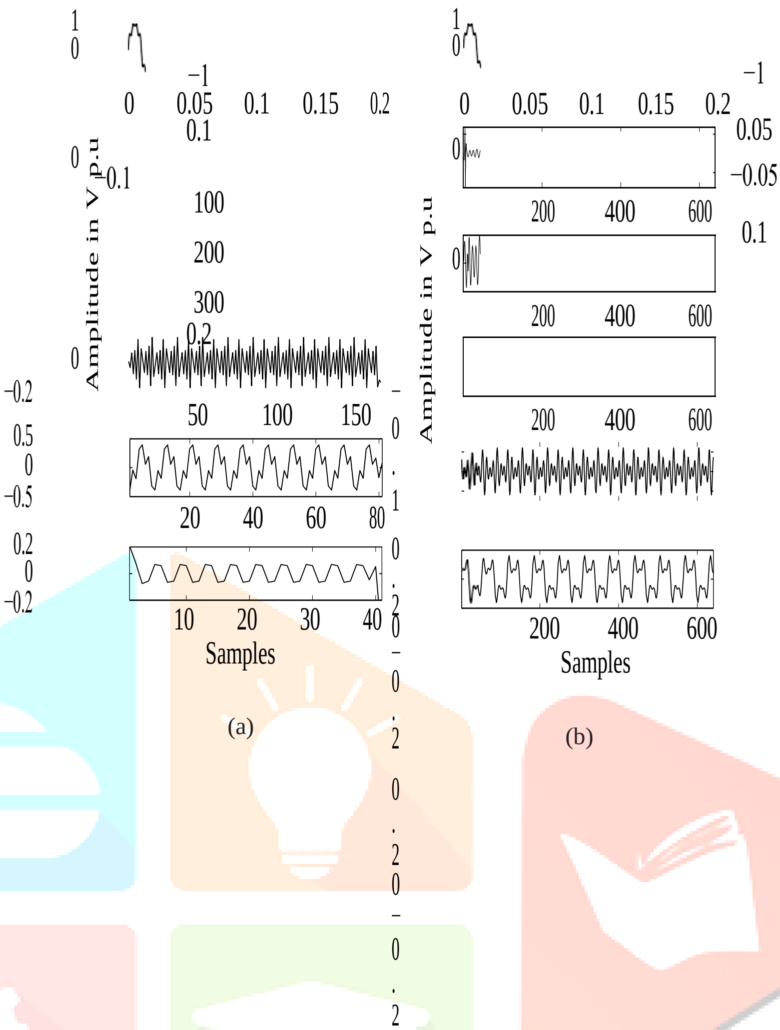

Fig. 7: Sine wave with Harmonic (a) DWT decomposition (b) MODWT decomposition TABLE II:

CA % of Pure Signals

Class	DT		RF	
	DWT %(CA)	MODWT %(CA)	DWT %(CA)	MODWT%(CA)
CL1	100	99.52	97.11	99.95
CL2	99.91	100	99.97	100
CL3	100	100	100	100
CL4	99.95	100	97.34	100
CL5	98.98	100	99.75	100
CL6	99.78	100	99.94	100
CL7	99.91	100	95.96	100
CL8	99.81	100	99.94	100
CL9	100	99.23	100	100
CL10	98.27	100	98.94	100
Total % CA	98.62	99.16	99.21	99.98

VII. RESULT OF THE CLASSIFICATION

The classification accuracy is computed by the automated classifiers described in Section-III. In this paper, total 31020 numbers of signals are simulated for the ten classes of disturbances and each of the signals are fed for decomposition up to seventh finer levels. So, each data set contains variable X ($X1$ standard deviation, $X2$ energy of details, $X3$ entropy, $X4$ CUSUM) and $L(L1, L2, \ldots, L7$ level of decomposition) which constitute 28 features. For each data set, 70% of the total data has been treated as the training data to build a training model and the rest 30% of data are apply for testing.

The pure PQD signal waveforms are added with the white Gaussian noise in order to realize the disturbances in the noisy environments. The data set with signal to noise ratio (SNR) of 20 dB. The Table II provides the calculated values of the %CA of all the ten classes using the two wavelet transform combined with the two classifiers in the noise free envirnment. The last row in the Table II is the average %CA of all the ten classes. Similar procedure has been realized for obtaining the classification accuracy of PQD signals (Table III).

Table II and Table III, have provided the classification accuracy of the PQD signals with the noisy and without noise environment. From the above Tables, it is observed that the RF classifier has better classification accuracy value than the DT.

TABLE III: CA % of Signals with 20 dB noise

Class	DT		RF	
	DWT %(CA)	MODWT %(CA)	DWT %(CA)	MODWT%(CA)
CL1	98.05	98.13	98.06	98.65
CL2	97.03	98.11	98.60	98.71
CL3	100	99.97	100	100
CL4	99.93	100	100	100
CL5	100	99.92	100	100
CL6	99.53	100	100	100
CL7	100	99.95	100	100
CL8	99.86	99.96	100	100
CL9	94.21	100	100	99.97
CL10	97.82	100	98.30	100
Total % CA	97.53	98.87	98.91	99.26

TABLE IV: CA % of three phase real time signal

Class	DT		RF	
	DWT %(CA)	MODWT %(CA)	DWT %(CA)	MODWT%(CA)
CL1	97.80	97.82	98.14	99.40
CL2	98.15	98.90	99.91	100
CL3	99.74	100	100	100
CL4	97.35	97.02	99.03	99.10
CL1+CL2	99.91	99.79	99.49	99.67
CL6	100	99.32	99.34	100
CL7	96.11	97.36	98.52	99.01
CL8	97.02	97.28	99.58	99.46
Total % CA	97.28	98.97	99.02	99.23

A. Classification with Real PQD signals

Eight different types of three phase PQD signals have been captured from an overhead power transmission line panel of length 360 km. The transmission demo panel comprises a line model of voltage of 380 kV. The equivalent circuit of the line is π model with concentrated parameters. The demo panel comprises of natural load 600 MW. A 380 V has been applied to transmission line panel and by changing the load and creating fault, the various disturbances are created like the single phase. These disturbances are then stored in a storage oscilloscope and fed to the MATLAB. The details of the experimental set up is given in Fig 8. These three phase signals have been fed to the aforementioned classifiers same as the previous cases.

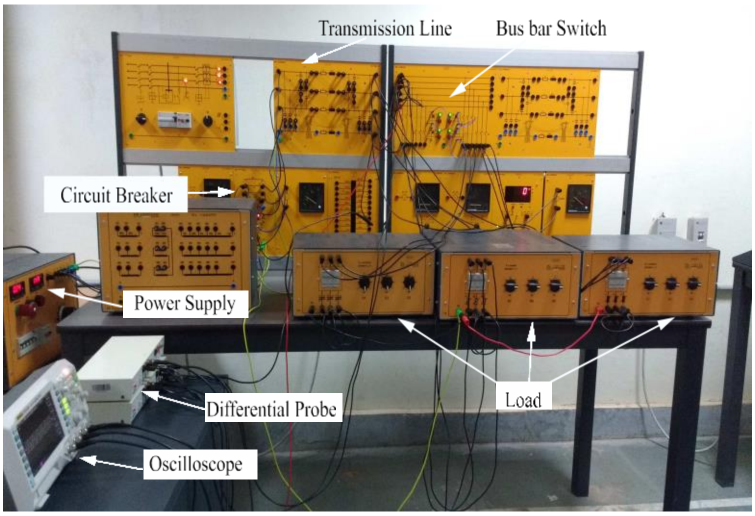

Fig. 8: Experimental setup for three phase voltage signal generation

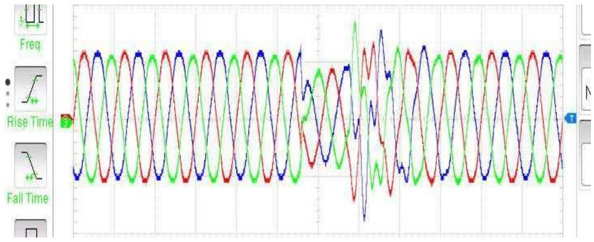

(a)

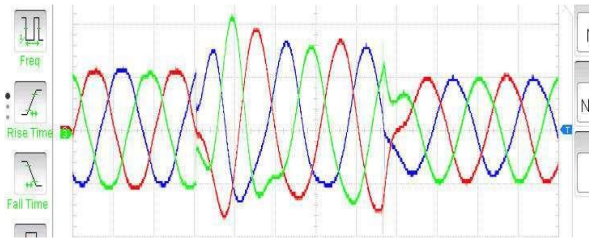

(b)

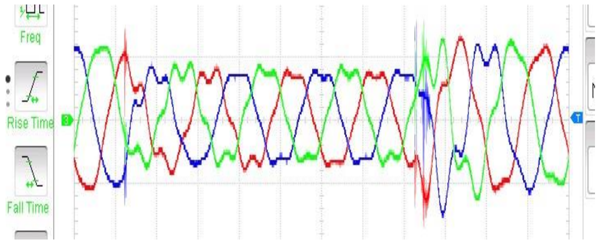

(c)

Fig. 9: Three phase real distorted voltage signals (a) Sag (b) Swell (c) Sag and harmonics

The classification of three phase PQ disturbances have been presented in Table IV. From Table IV, it can be observed that the aforementioned methods are working satisfactorily for the classification of real data. The RF classifier has provided good results compared to all other classifiers. Moreover $\%CA$ of MODWT based data set is very close to the DWT based data set just like that of the synthesized signal.

VIII. Conclusion

The useful features of the PQD signals have been extracted using the detail coefficients of the DWT and the MODWT decomposition. The classification accuracy of these simulated and the real signals have been obtained by MODWT as well as DWT with the combination of automatic classifiers such as DT and RF. From these aforementioned classifiers, it is observed that DWT has yielded similar classification accuracy like the MODWT. The down sampling free MODWT provides the proper localization of PQ disturbances along with the shifting. Elimination of down sampling overcomes the restriction in the choice of signal length. The insensitivity to the choice of starting point of time series has made MODWT as a suitable technique in real time environment. The ensemble decision has better classification rate than the single tree. However, RF classifies large data set satisfactorily where the DT fails due to over fitting. DT is extremely sensitive to small perturbations in the data set considered for analysis. Moreover, the RF also perform satisfactorily on real time environment.

References

[1] A. Gaouda, M. Salama, M. Sultan, and A. Chikhani, "Power quality detection and classification using wavelet-multiresolution signal decomposition," *IEEE Transactions on Power Delivery*, vol. 14, no. 4, pp. 1469–1476, 1999.

[2] L. Angrisani, P. Daponte, M. D'apuzzo, and A. Testa, "A measurement method based on the wavelet transform for power quality analysis," *Power Delivery, IEEE Transactions on*, vol. 13, no. 4, pp. 990–998, 1998.

[3] J. Douglas, "Solving problems of power quality," *EPRI Journal (Electric Power Research Institute);(United States)*, vol. 18, no. 8, 1993.

[4] D. Gabor, “Theory of communication. part 1: The analysis of information,” *Journal of the Institution of Electrical Engineers-Part III: Radio and Communication Engineering*, vol. 93, no. 26, pp. 429–441, 1946.
[5] B. Biswal, M. Biswal, S. Mishra, and R. Jalaja, “Automatic classification of power quality events using balanced neural tree,” *Industrial Electronics, IEEE Transactions on*, vol. 61, no. 1, pp. 521–530, 2014.
[6] R. A. Brown and R. Frayne, “A fast discrete s-transform for biomedical signal processing,” in *Engineering in Medicine and Biology Society, 2008. EMBS 2008. 30th Annual International Conference of the IEEE*, pp. 2586–2589, IEEE, 2008.
[7] T. Zafar and W. Morsi, “Power quality and the un-decimated wavelet transform: An analytic approach for time-varying disturbances,”
Electric Power Systems Research, vol. 96, pp. 201–210, 2013.
[8] A. Kumar, L. K. Joshi, A. Pal, and A. Shukla, “Modwt based time scale decomposition analysis of bse and nse indexes financial time series,”
[9] D. B. Percival and A. T. Walden, *Wavelet methods for time series analysis*, vol. 4. Cambridge University Press, 2006.
[10] A. S. Yilmaz, A. Subasi, M. Bayrak, V. M. Karsli, and E. Ercelebi, “Application of lifting based wavelet transforms to characterize power quality events,” *Energy conversion and management*, vol. 48, no. 1, pp. 112–123, 2007.
[11] S. Hasheminejad, S. Esmaeili, and S. Jazebi, “Power quality disturbance classification using s-transform and hidden markov model,” *Electric Power Components and Systems*, vol. 40, no. 10, pp. 1160–1182, 2012.
[12] M. Masoum, S. Jamali, and N. Ghaffarzadeh, “Detection and classification of power quality disturbances using discrete wavelet transform and wavelet networks,” *IET Science, Measurement & Technology*, vol. 4, no. 4, pp. 193–205, 2010.
[13] T. Abdel-Galil, E. El-Saadany, A. Youssef, and M. Salama, “Disturbance classification using hidden markov models and vector quantization,” *Power Delivery, IEEE Transactions on*, vol. 20, no. 3, pp. 2129–2135, 2005.
[14] R. Kohavi and J. R. Quinlan, “Data mining tasks and methods: Classification: decision-tree discovery,” in *Handbook of data mining and knowledge discovery*, pp. 267–276, Oxford University Press, Inc., 2002.
[15] H. Dehghani, B. Vahidi, R. Naghizadeh, and S. Hosseinian, “Power quality disturbance classification using a statistical and wavelet-based hidden markov model with dempster–shafer algorithm,” *International Journal of Electrical Power & Energy Systems*, vol. 47, pp. 368–377, 2013.
[16] K. S. Mwitondi, “Data mining with rattle and r,” *Journal of Applied Statistics*, vol. 40, no. 2, pp. 464–464, 2013.
[17] M. Biswal and P. K. Dash, “Detection and characterization of multiple power quality disturbances with a fast s-transform and decision tree based classifier,” *Digital Signal Processing*, vol. 23, no. 4, pp. 1071–1083, 2013.
[18] S. Santoso, E. J. Powers, W. M. Grady, and P. Hofmann, “Power quality assessment via wavelet transform analysis,” *Power Delivery, IEEE Transactions on*, vol. 11, no. 2, pp. 924–930, 1996.
[19] C. H. Kim and R. Aggarwal, “Wavelet transforms in power systems. i. general introduction to the wavelet transforms,” *Power Engineering Journal*, vol. 14, no. 2, pp. 81–87, 2000.
[20] T. Zhu, S. Tso, and K. Lo, “Wavelet-based fuzzy reasoning approach to power-quality disturbance recognition,” *Power Delivery, IEEE Transactions on*, vol. 19, no. 4, pp. 1928–1935, 2004.
[21] B. Biswal and S. Mishra, “Power signal disturbance identification and classification using a modified frequency slice wavelet transform,”
IET Generation, Transmission & Distribution, vol. 8, no. 2, pp. 353–362, 2014.
[22] M. Biswal and P. K. Dash, “Measurement and classification of simultaneous power signal patterns with an s-transform variant and fuzzy decision tree,” *Industrial Informatics, IEEE Transactions on*, vol. 9, no. 4, pp. 1819–1827, 2013.
[23] M. Mohammadi and G. Gharehpetian, “Application of core vector machines for on-line voltage security assessment using a decision-tree-based feature selection algorithm,” *IET generation, transmission & distribution*, vol. 3, no. 8, pp. 701–712, 2009.
[24] K. Thirumala, A. C. Umarikar, and T. Jain, “A generalized empirical wavelet transform for classification of power quality disturbances,” in *Power System Technology (POWERCON), 2016 IEEE International Conference on*, pp. 1–5, IEEE, 2016.
[25] R. Kumar, B. Singh, D. Shahani, A. Chandra, and K. Al-Haddad, “Recognition of power-quality disturbances using s-transform-based ann classifier and rule-based decision tree,” *IEEE Transactions on Industry Applications*, vol. 51, no. 2, pp. 1249–1258, 2015.
[26] G. J. Williams, “Rattle: a data mining gui for r,” *The R Journal*, vol. 1, no. 2, pp. 45–55, 2009.
[27] L. Breiman, “Random forests,” *Machine learning*, vol. 45, no. 1, pp. 5–32, 2001.
[28] S. Upadhyaya and S. Mohanty, “Power quality disturbance detection using wavelet based signal processing,” in *India Conference (INDICON), 2013 Annual IEEE*, pp. 1–6, IEEE, 2013.